

# The Enigma of the Highest Energy Particles of Nature

Günter Sigl

*GReCO, Institut d'Astrophysique de Paris, CNRS, 98bis Boulevard Arago,  
75014 Paris, France*

---

## Abstract

Historically cosmic rays have always been at the intersection of astrophysics with particle physics. This is still and especially true in current days where experimenters routinely observe atmospheric showers from particles whose energies reach macroscopic values up to about 50 Joules. This dwarfs energies achieved in the laboratory by about eight orders of magnitude in the detector frame and three orders of magnitude in the center of mass. While the existence of these highest energy cosmic rays does not necessarily testify physics not yet discovered, their macroscopic energies likely links their origin to the most energetic processes in the Universe. Explanations range from conventional shock acceleration to particle physics beyond the Standard Model and processes taking place at the earliest moments of our Universe. While motivation for some of the more exotic scenarios may have diminished by newest data, conventional shock acceleration scenarios remain to be challenged by the apparent isotropy of cosmic ray arrival directions which may not be easy to reconcile with a highly structured and magnetized Universe. Fortunately, many new experimental activities promise a strong increase of statistics at the highest energies and a combination with  $\gamma$ -ray and neutrino astrophysics will put strong constraints on all these theoretical models. This short review is far from complete and instead presents a selection of aspects regarded by the author as interesting and/or promising for the future.

---

## 1 Introduction

High energy cosmic ray (CR) particles are shielded by Earth's atmosphere and reveal their existence on the ground only by indirect effects such as ionization and showers of secondary charged particles covering areas up to many  $\text{km}^2$  for the highest energy particles. In fact, in 1912 Victor Hess discovered CRs by measuring ionization from a balloon [1], and in 1938 Pierre Auger proved the existence of extensive air showers (EAS) caused by primary particles with

energies above  $10^{15}$  eV by simultaneously observing the arrival of secondary particles in Geiger counters many meters apart [2].

After almost 90 years of CR research, their origin is still an open question, with a degree of uncertainty increasing with energy [3]: Only below 100 MeV kinetic energy, where the solar wind shields protons coming from outside the solar system, the sun must give rise to the observed proton flux. Above that energy the CR spectrum exhibits little structure and is approximated by broken power laws  $\propto E^{-\gamma}$ : At the energy  $E \simeq 4 \times 10^{15}$  eV called the “knee”, the flux of particles per area, time, solid angle, and energy steepens from a power law index  $\gamma \simeq 2.7$  to one of index  $\simeq 3.0$ . The bulk of the CRs up to at least that energy is believed to originate within the Milky Way Galaxy. Above the so called “ankle” at  $E \simeq 5 \times 10^{18}$  eV, the spectrum flattens again to a power law of index  $\gamma \simeq 2.8$ . This latter feature is often interpreted as a cross over from a steeper Galactic component, which above the ankle cannot be confined by the Galactic magnetic field, to a harder component of extragalactic origin.

Until the 1950s the energies achieved with experiments at accelerators were lagging behind observed CR energies which explains why many elementary particles such as the positron, the muon, and the pion were first discovered in CRs [4]. Today, where the center of mass (CM) energies observed in collisions with atmospheric nuclei reach up to a PeV, we have again a similar situation. In addition, CR interactions in the atmosphere predominantly occur in the extreme forward direction which allows to probe non-perturbative effects of the strong interaction. This is complementary to collider experiments where the detectors can only see interactions with significant transverse momentum transfer.

Over the last few years, several giant air showers have been detected both in ground detectors measuring the secondary shower particles directly in water tanks or scintillation counters [5,6] and in fluorescence telescopes detecting the nitrogen emission induced by the shower [7,8]. This confirms the arrival of CRs with energies up to a few hundred EeV ( $1 \text{ EeV} \equiv 10^{18} \text{ eV}$ ), corresponding to about 50 Joules. The existence of such ultra-high energy cosmic rays (UHECRs) poses a serious challenge for conventional theories of CR origin based on acceleration of charged particles in powerful astrophysical objects. The question of the origin of these UHECRs is, therefore, currently a subject of much theoretical research as well as experimental efforts. We refer to Ref. [9] for recent brief reviews, and Ref. [10,11] for detailed reviews.

The problems encountered in trying to explain UHECRs in terms of “bottom-up” acceleration mechanisms have been well-documented in a number of studies; see, e.g., Refs. [12–14]. In summary, apart from energy draining interactions in the source the maximal UHECR energy is limited by the product of the accelerator size and the strength of the magnetic field containing the

charged particles to be accelerated, similar to the situation in man-made accelerators such as at CERN. These criteria reveal that it is hard to accelerate protons and heavy nuclei up to the energies observed even in the most powerful astrophysical objects such as radio galaxies and active galactic nuclei.

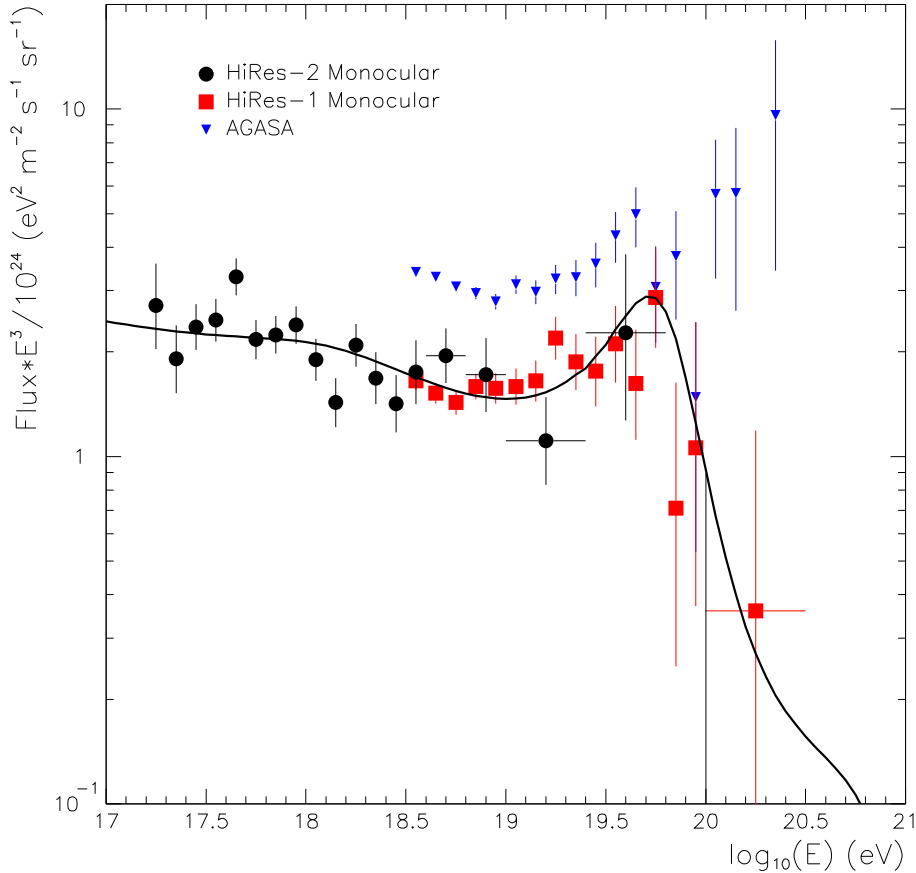


Fig. 1. UHECR flux as measured by the HiRes-I and HiRes-II detectors [8], and the AGASA experiment [6]. Also shown is a fit to the data of a superposition of a galactic and an extragalactic source component. This figure is from the second reference in Ref. [8].

In addition, nucleons above  $\simeq 70$  EeV lose energy drastically due to pion production on the cosmic microwave background (CMB) — the Greisen-Zatsepin-Kuzmin (GZK) effect [15] — which limits the distance to possible sources to less than  $\simeq 100$  Mpc [13]. Heavy nuclei at these energies are photodisintegrated in the CMB within a few Mpc [17]. If the sources are not too strongly clustered in our cosmologically local environment, a cut-off in the spectrum above  $\simeq 70$  EeV is therefore expected [16]. However, currently there seems to be a disagreement between the AGASA ground array [6] which detected about 8 events above  $10^{20}$  eV, as opposed to about 2 expected from a

cut-off, and the HiRes fluorescence detector [8] which seems consistent with a cut-off [20], see Fig. 1. The resolution of this problem may have to await the completion of the Pierre Auger project [21] which will combine these two complementary detection techniques.

Adding to the problem, there are no obvious astronomical counterparts within  $\simeq 100$  Mpc of the Earth [18,13]. At the same time, no significant large-scale anisotropy has been observed in UHECR arrival directions above  $\simeq 10^{18}$  eV, whereas there are strong hints for small-scale clustering: The AGASA experiment has observed five doublets and one triplet within  $2.5^\circ$  out of 57 events above 40 EeV [6]. This clustering has a chance probability of less than 1% in the case of an isotropic distribution.

There are currently two possible explanations of these experimental findings: The first one assumes negligible magnetic deflection. In this case most of the sources would have to be at cosmological distances which would explain the absence of nearby counterparts and the apparent isotropy would indicate that many sources contribute to the observed flux, where a subset of especially powerful sources would explain the small-scale clustering [19]. This scenario predicts the confirmation of a GZK cutoff. The second scenario is most likely more realistic and takes into account the likely existence of large scale intervening magnetic fields with intensity  $B \sim 0.1 - 1 \mu\text{G}$ , correlating with the large scale galaxy distribution. In this case magnetic deflection would be considerable even at the highest energies and the observed UHECR flux could be dominated by relatively few sources within about 100 Mpc. Here, large scale isotropy could be explained by considerable angular deflection leading to diffusion up to almost the highest energies and the small scale clustering could be due to magnetic lensing. This scenario will be discussed in section 3.

More speculative ways to explain the UHECR observations consist of circumventing the distance restriction imposed by the GZK effect by postulating either new particles or new interactions beyond the Standard Model of particle physics (section 4) or a violation of the Lorentz symmetry (section 5). These possibilities do not, however, solve the problem of acceleration to and beyond the observed energies which has to be solved separately.

In contrast, in the “top-down” scenarios, which will be discussed in section 6, the problem of energetics is trivially solved. Here, the UHECR particles are the decay products of some super-massive “X” particles of mass  $m_X \gg 10^{20}$  eV, and have energies all the way up to  $\sim m_X$ . Thus, no acceleration mechanism is needed. The massive X particles could be metastable relics of the early Universe with lifetimes of order of or above the current age of the Universe or could be released from topological defects (TDs) that were produced in the early Universe during symmetry-breaking phase transitions envisaged in Grand Unified Theories (GUTs). If the X particles themselves or their sources

cluster similar to dark matter, the dominant observable UHECR contribution would come from the Galactic Halo and absorption would be negligible. This option seems strongly constrained and may soon be ruled out.

Non-astrophysical solutions of the UHECR problem are of course in general quite model dependent. In addition, if the existence of the GZK cutoff will be confirmed, their motivation surely diminishes in general. On the other hand, even in this case UHECR can be used to test and constrain new physics beyond the Standard Model, such as new interactions beyond the reach of terrestrial accelerators (see section 4), violation of symmetries (see section 5), as well as Grand Unification and early Universe cosmology, such as the rate of TD and/or massive particle production in inflation (see section 6), at energies often inaccessible to accelerator experiments.

The physics and astrophysics of UHECRs are intimately linked with the emerging field of neutrino astronomy (for reviews see Refs. [22]) as well as with the already established field of  $\gamma$ -ray astronomy (for reviews see, e.g., Ref. [23]). Indeed, all scenarios of UHECR origin, including the top-down models, are severely constrained by neutrino and  $\gamma$ -ray observations and limits. In turn, this linkage has important consequences for theoretical predictions of fluxes of extragalactic neutrinos above about a TeV whose detection is a major goal of next-generation neutrino telescopes: If these neutrinos are produced as secondaries of protons accelerated in astrophysical sources and if these protons are not absorbed in the sources, but rather contribute to the UHECR flux observed, then the energy content in the neutrino flux can not be higher than the one in UHECRs, leading to the so called Waxman Bahcall bound for transparent sources with soft acceleration spectra [24,26]. If one of these assumptions does not apply, such as for acceleration sources with injection spectra harder than  $E^{-2}$  and/or opaque to nucleons, or in the top-down scenarios where X particle decays produce much fewer nucleons than  $\gamma$ -rays and neutrinos, the Waxman Bahcall bound does not apply, but the neutrino flux is still constrained by the observed diffuse  $\gamma$ -ray flux in the GeV range.

## 2 Propagation of Ultra-High Energy Radiation

Before discussing specific scenarios for the UHECR origin we give a short account of the interaction and energy loss processes relevant for the propagation of ultra-high energy cosmic and  $\gamma$ -rays, and neutrinos [27]. These processes have been implemented in various numerical codes used for computing spectra of all these particles [28–30]. In the following we assume a flat Universe with a Hubble constant of  $H = 70 \text{ km sec}^{-1}\text{Mpc}^{-1}$  and a cosmological constant  $\Omega_\Lambda = 0.7$ , as favored by current observations.

The relevant nucleon interactions are pair production by protons ( $p\gamma_b \rightarrow pe^-e^+$ ), photo-production of single or multiple pions ( $N\gamma_b \rightarrow N n\pi$ ,  $n \geq 1$ ), and neutron decay ( $n \rightarrow pe^-\bar{\nu}_e$ ). The nucleon threshold energy for single pion production on a background photon of energy  $\varepsilon$  is given by

$$E_{\text{th}} = \frac{m_\pi(m_N + m_\pi/2)}{\varepsilon} \simeq 6.8 \times 10^{16} \left(\frac{\varepsilon}{\text{eV}}\right)^{-1} \text{ eV}. \quad (1)$$

Typical CMB photon energies are  $\varepsilon \sim 10^{-3}$  eV, leading to the GZK “cutoff” at a few tens of EeV where the nucleon interaction length drops to about 6 Mpc.

$\gamma$ -rays and electrons/positrons initiate electromagnetic (EM) cascades on low energy radiation fields such as the CMB. The high energy photons undergo electron-positron pair production (PP;  $\gamma\gamma_b \rightarrow e^-e^+$ ). At energies below  $\sim 10^{14}$  eV photons interact mainly with the universal infrared and optical (IR/O) backgrounds, between  $\sim 10^{14}$  eV and  $\sim 100$  EeV mainly with the CMB, while above  $\sim 100$  EeV the main target is the universal radio background (URB). In the Klein-Nishina regime, where the CM energy is large compared to the electron mass, one of the outgoing particles usually carries most of the initial energy. This “leading” electron (positron) in turn can transfer almost all of its energy to a background photon via inverse Compton scattering (ICS;  $e\gamma_b \rightarrow e'\gamma$ ). EM cascades are driven by this cycle of PP and ICS. The energy degradation of the “leading” particle in this cycle is slow, whereas the total number of particles grows exponentially with time. Apart from these interactions of first order in the EM coupling, triplet pair production (TPP;  $e\gamma_b \rightarrow ee^-e^+$ ), and double pair production (DPP,  $\gamma\gamma_b \rightarrow e^-e^+e^-e^+$ ) can play a significant role in the formation of  $\gamma$ -ray spectrum in the energy range  $10^8 \text{ eV} < E < 10^{25} \text{ eV}$ . Finally, electrons are subject to synchrotron losses in large scale extragalactic magnetic fields (EGMF), whereas for protons synchrotron losses are negligible outside the sources.

Similarly to photons, ultra-high energy (UHE) neutrinos give rise to neutrino cascades in the primordial neutrino background via exchange of W and Z bosons [31]. Besides the secondary neutrinos which drive the neutrino cascade, the W and Z decay products include charged leptons and quarks which in turn feed into the EM and hadronic channels. Neutrino interactions become especially significant if the relic neutrinos have masses  $m_\nu$  in the eV range and thus constitute hot dark matter, because the Z boson resonance then occurs at an UHE neutrino energy  $E_{\text{res}} = 4 \times 10^{21}(\text{eV}/m_\nu) \text{ eV}$ . In fact, the decay products of this “Z-burst” have been proposed as a significant source of UHECRs [32]. The big drawback of this scenario is the need of enormous primary neutrino fluxes that cannot be produced by known astrophysical acceleration sources [29]. Even more exotic top-down type sources such as X particles decaying mostly into neutrinos appear ruled out due to a tendency to overproduce the diffuse GeV  $\gamma$ -ray flux observed by EGRET [33,30,34].

The two major uncertainties in the particle transport are the intensity and spectrum of the URB for which there exist no direct measurements in the relevant MHz regime [35,36], and the average value of the EGMF. Simulations have been performed for different assumptions on these uncertainties. A strong URB tends to suppress the UHE  $\gamma$ -ray flux by direct absorption whereas a strong EGMF blocks EM cascading (which otherwise develops efficiently especially in a low URB) by synchrotron cooling of the electrons. For the IR/O background we used the most recent data [37] for simulations in the present paper.

In top-down scenarios, the particle injection spectrum is generally dominated by the “primary”  $\gamma$ -rays and neutrinos over nucleons. These primary  $\gamma$ -rays and neutrinos are produced by the decay of the primary pions resulting from the hadronization of quarks that come from the decay of the X particles. In contrast, in acceleration scenarios the primaries are accelerated protons or nuclei, and  $\gamma$ -rays, electrons, and neutrinos are produced as secondaries from decaying pions that are in turn produced by the interactions of nucleons with the low energy photon background.

### 3 Deflection in Cosmic Magnetic Fields and the Anisotropy Problem

Magnetic fields are omnipresent in the Universe, but their origin still lies in the dark [38]. Best known are the magnetic fields in galaxies which have strengths of a few micro Gauss, but there are also some indications for fields correlated with larger structures such as galaxy clusters [39]. Magnetic fields as strong as  $\simeq 1\mu G$  in sheets and filaments of the large scale galaxy distribution, such as in our Local Supercluster, are compatible with existing upper limits on Faraday rotation [39–41]. It is also possible that fossil cocoons of former radio galaxies, so called radio ghosts, contribute to the isotropization of UHECR arrival directions [42].

Contrary to the case of electrons, for charged hadrons deflection is more important than synchrotron loss in the EGMF. To get an impression of typical deflection angles one can characterize the EGMF by its r.m.s. strength  $B$  and a coherence length  $l_c$ . If we neglect energy loss processes for the moment, then the r.m.s. deflection angle over a distance  $r$  in such a field is  $\theta(E, r) \simeq (2rl_c/9)^{1/2}/r_L$  [43], where the Larmor radius of a particle of charge  $Ze$  and energy  $E$  is  $r_L \simeq E/(ZeB)$ . In numbers this reads

$$\theta(E, r) \simeq 0.8^\circ Z \left( \frac{E}{10^{20} \text{ eV}} \right)^{-1} \left( \frac{r}{10 \text{ Mpc}} \right)^{1/2} \left( \frac{l_c}{1 \text{ Mpc}} \right)^{1/2} \left( \frac{B}{10^{-9} \text{ G}} \right), \quad (2)$$

for  $r \gtrsim l_c$ . This expression makes it immediately obvious why a magnetized Local Supercluster with fields of fractions of micro Gauss prevents a direct assignment of sources in the arrival directions of observed UHECRs; the deflection expected is many tens of degrees even at the highest energies. This goes along with a time delay  $\tau(E, r) \simeq r\theta(E, d)^2/4 \simeq 1.5 \times 10^3 Z^2 (E/10^{20} \text{ eV})^{-2} (r/10 \text{ Mpc})^2 (l_c/\text{Mpc})(B/10^{-9} \text{ G})^2 \text{ yr}$  which can be millions of years. A source visible in UHECRs today could therefore be optically invisible since many models involving, for example, active galaxies as UHECR accelerators, predict variability on shorter time scales.

On the other hand, an EGMF of this size could explain the observed large scale UHECR isotropy by diffusion and the small-scale clustering by magnetic lensing, even if most of the sources are relatively nearby. In fact, numerical simulations of nucleons in a simplified scenario where the UHECR source density in the Local Supercluster is idealized as a Gaussian sheet of a few Mpc thickness and about 20 Mpc length containing a magnetic field with a Kolmogorov spectrum and an r.m.s. strength  $B$  proportional to the same profile have lead to the following result: About 10 sources in the Local Supercluster and a maximal field strength of  $\simeq 0.3\mu \text{ G}$  lead to arrival direction multi-pole moments and autocorrelation functions consistent with the AGASA data [44].

Most recent results indicate that the situation is similar in more realistic models of the Local Supercluster. We have used the  $(50 \text{ Mpc})^3$  box of a large scale structure simulation [45] where the magnetic field was followed passively and normalized to the known strengths of a few micro Gauss in the center of galaxy clusters. In this simulated box we selected as observer a place typical for our neighborhood in the Local Supercluster, and chose randomly a certain number of sources with probability proportional to the local baryon density. For each such configuration 5000 nucleon trajectories originating from the sources (assumed to emit equal spectra and power) and reaching the observer were computed numerically, taking into account energy losses and deflection in the magnetic field in the box. For each realization these 5000 trajectories were used to construct arrival direction probability distributions taking into account the solid-angle dependent exposure function for the respective experiment and folding over the angular resolution. From these distributions mock data sets consisting of  $N$  observed events were dialed. For each such mock data set or for the real data set we then obtained estimators for the spherical harmonic coefficients  $C(l)$  and the autocorrelation function  $N(\theta)$ . The estimator for  $C(l)$  is defined as

$$C(l) = \frac{1}{2l+1} \frac{1}{\mathcal{N}^2} \sum_{m=-l}^l \left( \sum_{i=1}^N \frac{1}{\omega_i} Y_{lm}(u^i) \right)^2, \quad (3)$$

where  $\omega_i$  is the total experimental exposure at arrival direction  $u^i$ ,  $\mathcal{N} =$



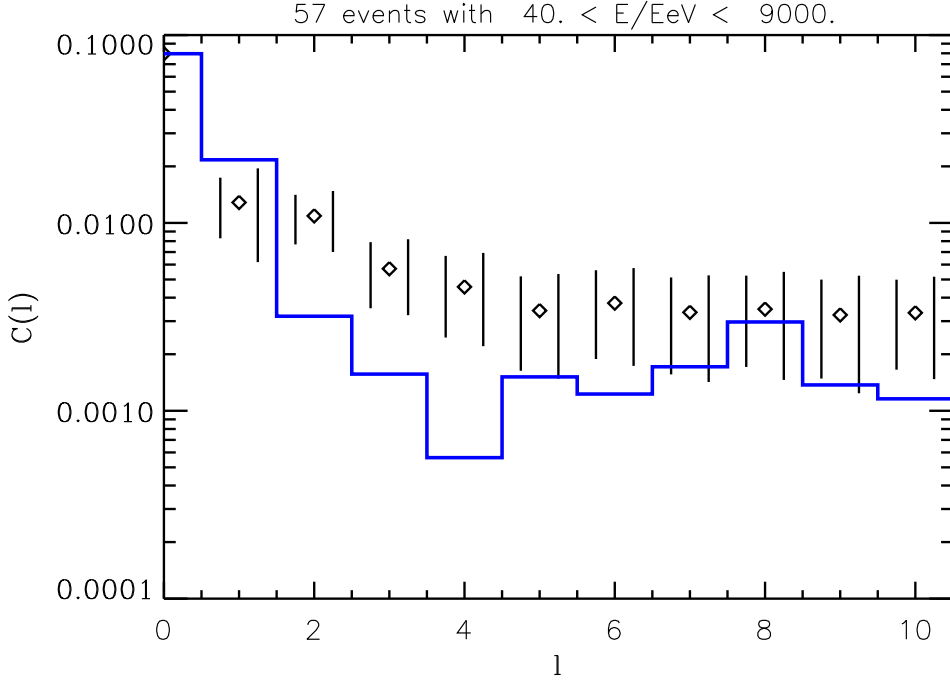


Fig. 2. The angular power spectrum  $C(l)$  as a function of multi-pole  $l$ , obtained for the AGASA exposure function, for  $N = 57$  events observed above 40 EeV, sampled from 12 simulated configurations of 100 sources in the simulation box of Ref. [45], emitting a proton spectrum  $\propto E^{-2.4}$  up to  $10^{21}$  eV. The magnetic field strength at the observer is  $\simeq 0.13\mu\text{G}$ . The diamonds indicate the average over 12 realizations, and the left and right error bars represent the statistical and total (including cosmic variance due to different realizations) error, respectively, see text for explanations. The histogram represents the AGASA data. The overall likelihood significance is  $\simeq 0.15$ .

$\sum_{i=1}^N 1/\omega_i$  is the sum of the weights  $1/\omega_i$ , and  $Y_{lm}(u^i)$  is the real-valued spherical harmonics function taken at direction  $u^i$ . The estimator for  $N(\theta)$  is defined as

$$N(\theta) = \frac{1}{2S(\theta)} \sum_{j \neq i} \left\{ \begin{array}{l} 1 \text{ if } \theta_{ij} \text{ is in same bin as } \theta \\ 0 \text{ otherwise} \end{array} \right\}, \quad (4)$$

and  $S(\theta)$  is the solid angle size of the corresponding bin.

The different mock data sets in the various realizations yield the statistical distributions of  $C(l)$  and  $N(\theta)$ . One defines the average over all mock data sets and realizations as well as two errors: The smaller error (shown to the left of the average in Figs. 2 and 3) is the statistical error, i.e. the fluctuations due to the finite number  $N$  of observed events, averaged over all realizations, while the larger error (shown to the right of the average in Figs. 2 and 3) is the “total

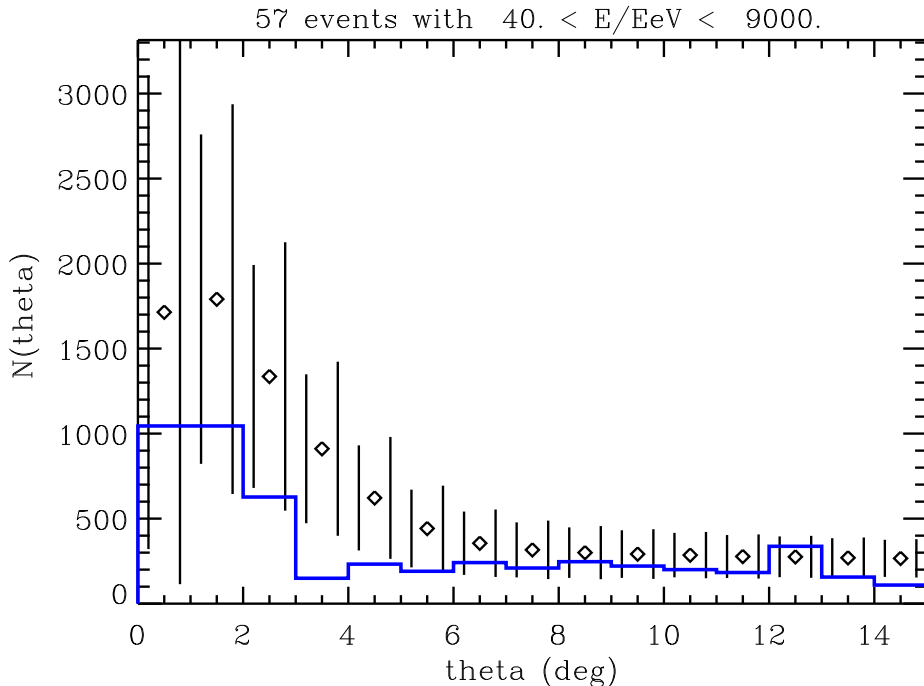


Fig. 3. As Fig. 2, but for the angular correlation function  $N(\theta)$  as a function of angular distance  $\theta$ , using a bin size of  $\Delta\theta = 1^\circ$ . The overall likelihood significance is  $\simeq 0.63$ .

error”, i.e. the statistical error plus the cosmic variance, in other words, the fluctuations due to finite number of events and the variation between different realizations of observer and source positions. For a given data set a  $\chi^2$  summed over all bins can be defined relative to the mean and variance of  $C(l)$  and  $N(\theta)$  simulated for a given model. From this one can obtain an overall likelihood for the consistency of a given real data set with a given model by counting the fraction of simulated mock data sets with a  $\chi^2$  larger than for the real data.

We find that as long as the observer is surrounded by magnetic fields above about  $0.1\mu\text{G}$ , which is possible but not obvious for our environment, roughly 10 or more sources lead to multi-poles and autocorrelations marginally consistent with present data which are limited to the Northern hemisphere, although consistency of large scale multi-poles is somewhat worse than for more extended EGMFs. An example for 100 sources is shown in Figs. 2 and 3 [46]. A proton injection spectrum roughly  $\propto E^{-2.4}$  extending up to  $\simeq 10^{21}$  eV can reproduce the sub-GZK spectrum and tends to predict a spectrum somewhere between the AGASA and HiRes observations above GZK energies, see Fig. 4. In contrast, if the observer is in a region of EGMF field strength much smaller than  $\simeq 0.1\mu\text{G}$ , the UHECR sky distribution reflects the highly structured large scale galaxy distribution and is thus inconsistent with the observed isotropy.

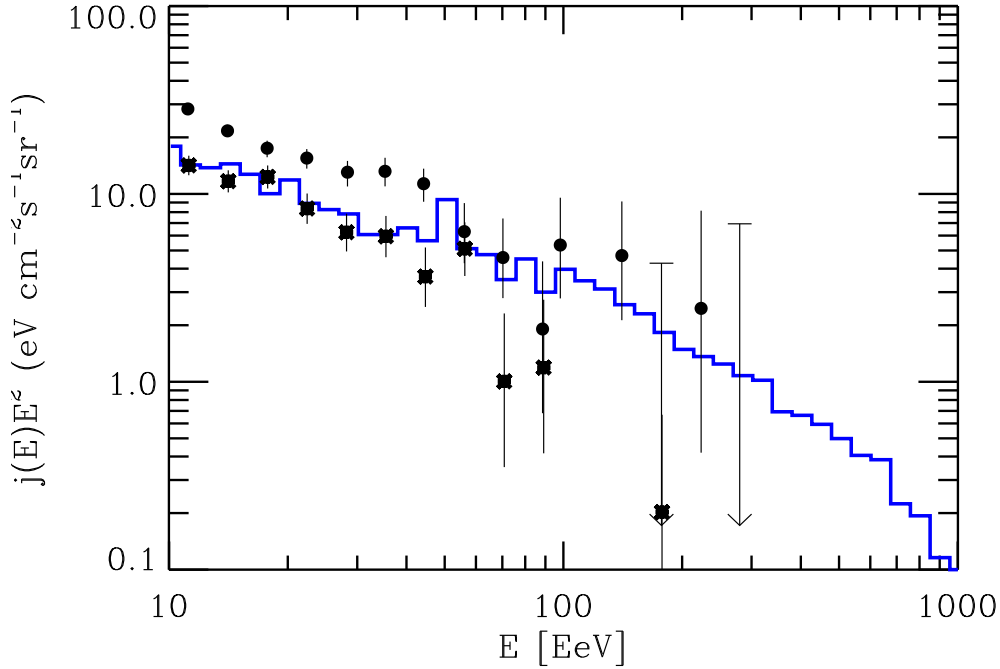


Fig. 4. Predicted spectrum observable by AGASA for the scenario discussed in the text and shown in Figs. 2 and 3, averaged over 12 realizations, as compared to the AGASA (dots) and HiRes-I (stars) data.

We also find that sources outside our Local Supercluster do not contribute significantly to the observable flux if the observer is immersed in magnetic fields above about  $0.1\mu\text{G}$  and if sources reside in magnetized clusters and superclusters: For particles above the GZK cutoff this is because sources outside the Local Supercluster are beyond the GZK distance. Sub-GZK particles are mainly contained in the magnetized environment of their sources and thus exhibit a much higher local over-density than their sources. Further, the suppressed flux of low energy particles leaving their environment is largely kept out of our Local Supercluster by its own magnetic field [44]. Both effects can be understood qualitatively by matching the flux  $j(E)$  in the unmagnetized region with the diffusive flux  $-D(E)\nabla n(E, \mathbf{r})$  in terms of the diffusion constant  $D(E)$  and the density  $n(E, \mathbf{r})$  of particles of energy  $E$  which shows that the density gradient always points to the source. A significant contribution from sources at cosmological distance would require magnetic fields in the nano Gauss range, and even then would be unlikely to explain the observed clustering.

The confidence levels that can be obtained with this method for specific models of our local magnetic and UHECR source neighborhood will greatly increase with the increase of data anticipated from future experiments. Full sky coverage alone will play an important role in this context as many scenarios

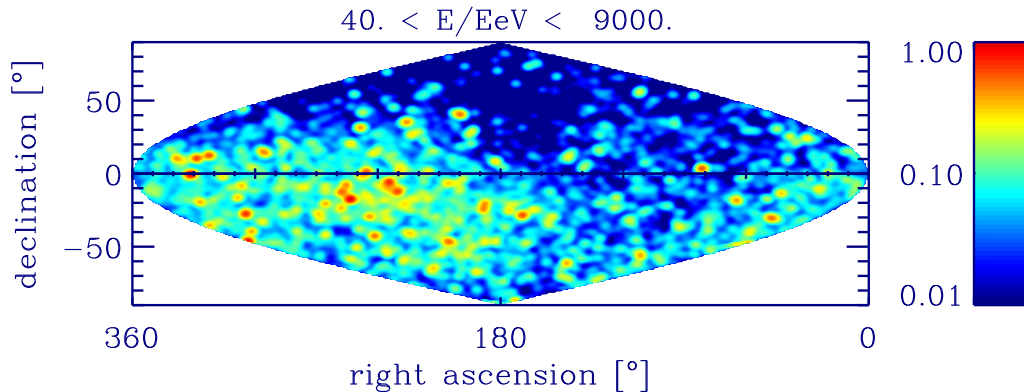


Fig. 5. The UHECR arrival direction distribution above 40 EeV in terrestrial coordinates for the scenario of Figs. 2–4, averaged over all 12 realizations of 5000 trajectories each. The color scale represents the integral flux per solid angle. The pixel size is  $1^\circ$  and the image has been convolved to an angular resolution of  $2.4^\circ$  corresponding to the approximate AGASA angular resolution.

predict large dipoles for the UHECR distribution. This is the case for the specific simulation box on which Figs. 2–4 are based, as demonstrated in Fig. 5. Whereas current northern hemisphere data are consistent with this scenario at the  $\simeq 1.5$  sigma level, a comparable or larger exposure in the southern hemisphere would be sufficient in this case to find a dipole at several sigma confidence level.

Modeling our cosmic neighborhood and simulating UHECR propagation in this environment will therefore become more and more important in the coming years. This will also have to include the effects of the Galactic magnetic field and an extension to a possible heavy component of nuclei. For first steps in this direction see, e.g. Ref. [47] and Ref. [48], respectively.

#### 4 New Primary Particles and Interactions

A possible way around the problem of missing counterparts within acceleration scenarios is to propose primary particles whose range is not limited by interactions with the CMB. Within the Standard Model the only candidate is the neutrino, whereas in extensions of the Standard Model one could think of new neutrals such as axions or stable supersymmetric elementary particles. Such options are mostly ruled out by the tension between the necessity of a small EM coupling to avoid the GZK cutoff and a large hadronic coupling to ensure normal air showers [49]. Also suggested have been new neutral hadronic bound states of light gluinos with quarks and gluons, so-called R-hadrons that are heavier than nucleons, and therefore have a higher GZK threshold [50], as

can be seen from Eq. (1). Since this too seems to be disfavored by accelerator constraints [51] we will here focus on neutrinos.

In both the neutrino and new neutral stable particle scenario the particle propagating over extragalactic distances would have to be produced as a secondary in interactions of a primary proton that is accelerated in a powerful active galactic nucleus which can, in contrast to the case of EAS induced by nucleons, nuclei, or  $\gamma$ -rays, be located at high redshift. Consequently, these scenarios predict a correlation between primary arrival directions and high redshift sources. In fact, possible evidence for a correlation of UHECR arrival directions with compact radio quasars and BL-Lac objects, some of them possibly too far away to be consistent with the GZK effect, was recently reported [52]. The main challenge in these correlation studies is the choice of physically meaningful source selection criteria and the avoidance of a posteriori statistical effects. However, a moderate increase in the observed number of events will most likely confirm or rule out the correlation hypothesis. Note, however, that these scenarios require the primary proton to be accelerated up to at least  $10^{21}$  eV, demanding a very powerful astrophysical accelerator.

#### 4.1 New Neutrino Interactions

Neutrino primaries have the advantage of being well established particles. However, within the Standard Model their interaction cross section with nucleons, whose charged current part can be parametrized by [53]

$$\sigma_{\nu N}^{SM}(E) \simeq 2.36 \times 10^{-32} (E/10^{19} \text{ eV})^{0.363} \text{ cm}^2, \quad (5)$$

for  $10^{16} \text{ eV} \lesssim E \lesssim 10^{21} \text{ eV}$ , falls short by about five orders of magnitude to produce air showers as they are observed. However, it has been suggested that the neutrino-nucleon cross section,  $\sigma_{\nu N}$ , can be enhanced by new physics beyond the electroweak scale in the CM frame, or above about a PeV in the nucleon rest frame. Neutrino induced air showers may therefore rather directly probe new physics beyond the electroweak scale.

One possibility consists of a large increase in the number of degrees of freedom above the electroweak scale [54]. A specific instance of this idea appears in theories with  $n$  additional large compact dimensions and a quantum gravity scale  $M_{4+n} \sim \text{TeV}$  that has recently received much attention in the literature [55] because it provides an alternative solution to the hierarchy problem in grand unifications of gauge interactions without a need of supersymmetry. One of the largest contributions to the neutrino-nucleon cross section turns out to be the production on the brane representing our world of microscopic black holes which extend into the extra dimensions. The production of compact

branes, completely wrapped around the extra dimensions, may provide even larger contributions [56]. The cross sections can be larger than in the Standard model one by up to a factor  $\sim 100$  for reasonable parameters [57]. However, this is not sufficient to explain the observed UHECR events [58].

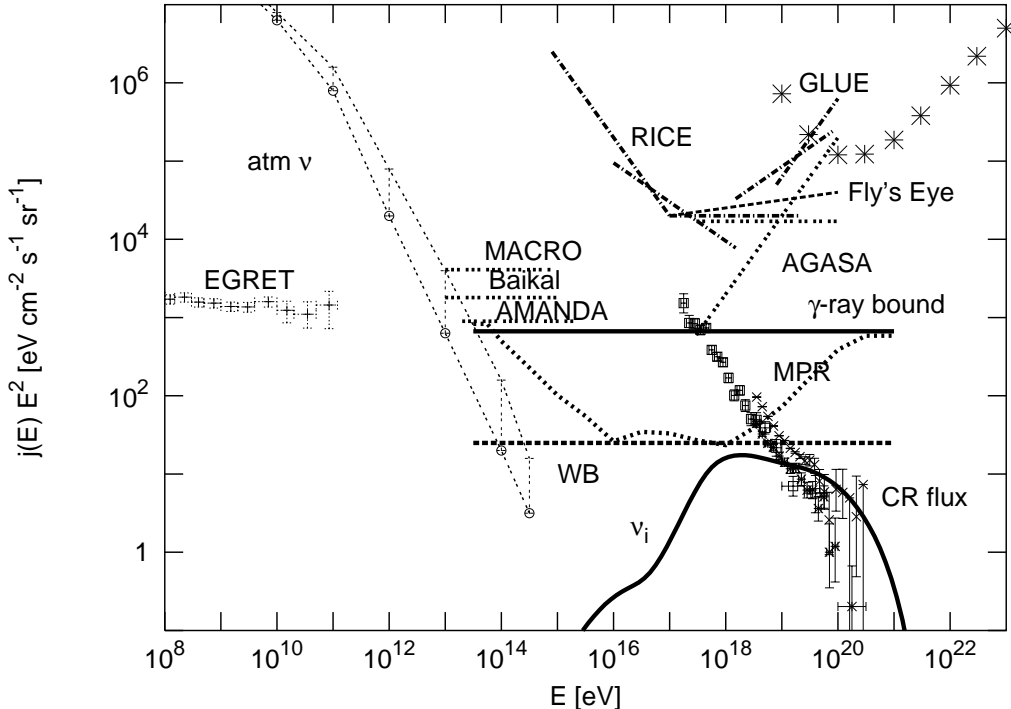


Fig. 6. [59] Cosmogenic neutrino flux per flavor (thick line, assuming maximal mixing among all flavors) produced by primary proton flux from the AGASA [6] and HiRes [8] experiments above  $3 \times 10^{18}$  eV (error bars). The UHECR sources were assumed to inject a proton spectrum  $\propto E^{-2}$  up to  $10^{22}$  eV with luminosity  $\propto (1+z)^3$  up to  $z = 2$ . For comparison shown are the atmospheric neutrino flux [60], as well as existing upper limits on the diffuse neutrino fluxes from MACRO [61], AMANDA [62], BAIKAL [63], AGASA [64], the Fly’s Eye [65] and RICE [66] experiments, and the limit obtained with the Goldstone radio telescope (GLUE) [67], as indicated. Theoretical neutrino flux upper limits based on the  $\gamma$ -ray bound derived from the EGRET diffuse  $\gamma$ -ray flux (shown on left part between 30 MeV and 100 GeV) [33], the MPR limit for optically thin sources [26], and the WB limit for AGN-like redshift evolution [24] are also shown.

However, the UHECR data can be used to put constraints on cross sections satisfying  $\sigma_{\nu N}(E \gtrsim 10^{19} \text{ eV}) \lesssim 10^{-27} \text{ cm}^2$ . Particles with such cross sections would give rise to horizontal air showers which have not yet been observed. Resulting upper limits on their fluxes assuming the Standard Model cross section Eq. (5) are shown in Fig. 6. Comparison with the “cosmogenic” neutrino flux produced by UHECRs interacting with the CMB then results in upper limits on the cross section which are about a factor 1000 larger than Eq. (5) in the energy range between  $\simeq 10^{17}$  eV and  $\simeq 10^{19}$  eV [68–70]. The projected sensitivity of future experiments shown in Fig. 7 below indicate that these

limits could be lowered down to the Standard Model one [70]. In case of a detection of penetrating events the degeneracy of the cross section with the unknown neutrino flux could be broken by comparing the rates of horizontal air showers with the ones of Earth skimming events [71].

The CM energy reached by an UHECR nucleon of energy  $E$  interacting with an atmospheric nucleon at rest is  $\sqrt{s} \simeq 0.4(E/10^{20} \text{ eV}) \text{ PeV}$ . Since the starting points in the atmosphere of observed EAS at these energies are consistent with normal hadronic cross sections, scenarios predicting dramatic increases or saturation of cross sections in the TeV range can probably be excluded. It is generally expected that new physics appears at TeV scales, and dramatic effects are possible when this scale is related to a true fundamental gravity scale. There are, for example, string-inspired scenarios with infinite-volume extra dimensions and a string scale  $M_s \simeq M_{\text{eff}}^2/M_{\text{Pl}} \sim (M_{\text{eff}}/TeV)^2 10^{-3} \text{ eV}$ , where  $M_{\text{eff}}$  is the energy scale where cross sections would undergo a Hagedorn-like saturation [72,73], and  $M_{\text{Pl}} \simeq 1.72 \times 10^{18} \text{ GeV}$  is the reduced Planck mass. The UHECR argument would then require  $M_{\text{eff}} \gtrsim \text{PeV}$  and thus  $M_s \gtrsim 100 \text{ eV}$ . However, in case of at least two infinite extra dimensions gravity would appear higher-dimensional, i.e. decreasing with a higher power of distance than Newtonian gravity on scales  $r \gtrsim M_{\text{Pl}}/M_s^2 \simeq 1 \text{ pc} (M_s/100\text{eV})^{-2}$ . The above bound would thus imply modifications of gravity on parsec scales which seems phenomenologically inviable. This is an example where UHECR observations can constrain models not constrained yet by collider physics due to the lower CM energies reached. Of course, UHECR observations are much more indirect and thus are only sensitive to dramatic effects such as Hagedorn saturation and macroscopic cross sections [74].

## 5 Violation of Lorentz Invariance

The most elegant solution to the problem of apparently missing nearby sources of UHECRs and for their putative correlation with high redshift sources would be to speculate that the GZK effect does not exist theoretically. A number of authors pointed out [75,76] that this may be possible by allowing violation of Lorentz invariance (VLI) by a tiny amount that is consistent with all current experiments. At a purely theoretical level, several quantum gravity models including some based on string theories do in fact predict non-trivial modifications of space-time symmetries that also imply VLI at extremely short distances (or equivalently at extremely high energies); see e.g., Ref. [77] and references therein. These theories are, however, not yet in forms definite enough to allow precise quantitative predictions of the exact form of the possible VLI. Current formulations of the effects of a possible VLI on high energy particle interactions relevant in the context of UHECR, therefore, adopt a phenomenological approach in which the form of the possible VLI is parametrized in var-

ious ways. VLI generally implies the existence of a universal preferred frame which is usually identified with the frame that is comoving with the expansion of the Universe, in which the CMB is isotropic.

A direct way of introducing VLI is through a modification of the standard *dispersion relation*,  $E^2 - p^2 = m^2$ , between energy  $E$  and momentum  $p = |\vec{p}|$  of particles,  $m$  being the invariant mass of the particle. Currently there is no unique way of parameterizing the possible modification of this relation in a Lorentz non-invariant theory. We discuss here a parametrization of the modified dispersion relation which covers most of the qualitative cases discussed in the literature and, for certain parameter values, allows to completely evade the GZK limit,

$$E^2 - p^2 - m^2 \simeq -2dE^2 - \xi \frac{E^3}{M_{\text{Pl}}} - \zeta \frac{E^4}{M_{\text{Pl}}^2}. \quad (6)$$

Here, the Planck mass  $M_{\text{Pl}}$  characterizes non-renormalizable effects with dimensionless coefficients  $\xi$  and  $\zeta$ , and the dimensionless constant  $d$  exemplifies VLI effects due to renormalizable terms in the Lagrangian. The standard Lorentz invariant dispersion relation is recovered in the limit  $\xi, \zeta, d \rightarrow 0$ . In critical string theory, effects second order in  $M_{\text{Pl}}^{-1}$ ,  $\zeta \neq 0$ , can be induced due to quantum gravity effects. The constants  $d \neq 0$  can break Lorentz invariance spontaneously when certain Lorentz tensors  $c_{\mu\nu}$  have couplings to fermions of the form  $d_{\mu\nu} \bar{\psi} \gamma^\mu \partial^\nu \psi$ , and acquire vacuum expectation values of the form  $\langle d_{\mu\nu} \rangle = d \delta_\mu^0 \delta_\nu^0$  [79]. Effects of first order in  $M_{\text{Pl}}^{-1}$ ,  $\xi \neq 0$ , are possible, for example, in non-critical Liouville string theory due to recoiling D-branes [80].

Now, consider the GZK photo-pion production process in which a nucleon of energy  $E$ , momentum  $p$  and mass  $m_N$  collides head-on with a CMB photon of energy  $\epsilon$  producing a pion and a recoiling nucleon. The threshold initial momentum of the nucleon for this process according to standard Lorentz invariant kinematics is

$$p_{\text{th},0} = (m_\pi^2 + 2m_\pi m_N)/4\epsilon, \quad (7)$$

where  $m_\pi$  and  $m_N$  are the pion and nucleon masses, respectively. Assuming exact energy-momentum conservation but using the modified dispersion relation given above, in the ultra-relativistic regime  $m \ll p \ll M$ , and neglecting sub-leading terms, the new nucleon threshold momentum  $p_{\text{th}}$  under the modified dispersion relation Eq. (6) for  $d = 0$  satisfies [81]

$$-\beta x^4 - \alpha x^3 + x - 1 = 0, \quad (8)$$

where  $x = p_{\text{th}}/p_{\text{th},0}$ , and



$$\alpha = \frac{2\xi p_{\text{th},0}^3}{(m_\pi^2 + 2m_\pi m_N)M_{\text{Pl}}} \frac{m_\pi m_N}{(m_\pi + m_N)^2} \quad (9)$$

$$\beta = \frac{3\zeta p_{\text{th},0}^4}{2(m_\pi^2 + 2m_\pi m_N)M_{\text{Pl}}^2} \frac{m_\pi m_N}{(m_\pi + m_N)^2}.$$

One can show that the same modified dispersion relation Eq. (6) leads to the same condition Eq. (8) for absorption of high energy gamma rays through  $e^+e^-$  pair production on the infrared, microwave or radio backgrounds, if one substitutes  $p_{\text{th},0} = m_e^2/\epsilon$ ,  $\alpha = \xi p_{\text{th},0}^3/(8m_e^2 M_{\text{Pl}})$ ,  $\beta = 3\zeta p_{\text{th},0}^4/(16m_e^2 M_{\text{Pl}}^2)$ , where  $m_e$  is the electron mass.

If  $\xi, \zeta \simeq 1$ , there is no real positive solution of Eq. (8), implying that the GZK process does not take place and consequently the GZK cutoff effect disappears completely. Thus UHE nucleons and/or photons will be able to reach Earth from any distance. On the other hand, if future UHECR data confirm the presence of a GZK cutoff at some energy then that would imply upper limits on the couplings  $\xi$  and  $\zeta$ , thus probing specific Lorentz non-invariant theories. If  $p_{\text{th}} \simeq p_{\text{th},0}$ , one could conclude from Eq. (8) that  $\alpha, \beta \lesssim 1$ , which translates into  $|\xi| \lesssim 10^{-13}$  for the first order effects, and  $|\zeta| \lesssim 10^{-6}$  for the second order effects,  $\xi = 0$  [81]. Confirmation of a cut-off for TeV photons with next-generation  $\gamma$ -ray observatories would lead to somewhat weaker constraints [82].

In addition, the non-renormalizable terms in the dispersion relation Eq. (6) imply a change in the group velocity which for the first-order term leads to time delays over distances  $r$  given by

$$\Delta t \simeq \xi r \frac{E}{M_{\text{Pl}}} \simeq \xi \left( \frac{r}{100 \text{ Mpc}} \right) \left( \frac{E}{\text{TeV}} \right) \text{ sec}. \quad (10)$$

For  $|\xi| \sim 1$  such time delays could be measurable, for example, by fitting the arrival times of  $\gamma$ -rays arriving from  $\gamma$ -ray bursts to the predicted energy dependence.

We mention that if VLI is due to modification of the space-time structure expected in some theories of quantum gravity, for example, then the strict energy-momentum conservation assumed in the above discussion, which requires space-time translation invariance, is not guaranteed in general, and then the calculation of the modified particle interaction thresholds becomes highly non-trivial and non-obvious. Also, it is possible that a Lorentz non-invariant theory while giving a modified dispersion relation also imposes additional kinematic structures such as a modified law of addition of momenta. Indeed, Ref. [77] gives an example of a so-called  $\kappa$ -Minkowski non-commutative space-time in which the modified dispersion relation has the same form as in Eq. (6) but there is also a modified momentum addition rule which compen-

sates for the effect of the modified dispersion relation on the particle interaction thresholds discussed above leaving the threshold momentum unaffected and consequently the GZK problem unsolved. In scenarios where the relativity of inertial frames is preserved by a non-linear representation of the Poincaré group, thresholds are in general significantly modified only if the effective mass scale  $M_{\text{Pl}}/xi$  is of the order of the unmodified threshold energy in the laboratory frame [78].

VLI by dimensionless terms such as  $d$  in Eq. (6) has been considered in Ref. [76]. These terms are obtained by adding renormalizable terms that break Lorentz invariance to the Standard Model Lagrangian. The dimensionless terms can be interpreted as a change of the maximal particle velocity  $v_{\text{max}} = \partial E/\partial p|_{E,p \gg m} \simeq 1 - d$ . At a fixed energy  $E$  one has the correspondence  $d \rightarrow (\xi/2)(E/M_{\text{Pl}}) + (\zeta/2)(E/M_{\text{Pl}})^2$ , as can be seen from Eq. (6). The above values for  $\xi$  and  $\zeta$  influencing the GZK effect then translate into values  $|d| \gtrsim 10^{-24}$ .

There are several other fascinating effects of allowing a small VLI, some of which are relevant for the question of origin and propagation of UHECR, and the resulting constraints on VLI parameters from cosmic ray observations are often more stringent than the corresponding laboratory limits; for more details, see Ref. [76] and [83].

## 6 Top-Down Scenarios

The difficulties of bottom-up acceleration scenarios discussed earlier motivated the proposal of the “top-down” scenarios, where UHECRs, instead of being accelerated, are the decay products of certain “X” particles of mass close to the GUT scale. Such particles can be produced in basically two ways: If they are very short lived, as usually expected in many GUTs, they have to be produced continuously. The only way this can be achieved is by emission from TDs left over from cosmological phase transitions that may have occurred in the early Universe at temperatures close to the GUT scale, possibly during reheating after inflation. TDs necessarily occur between regions that are causally disconnected, such that the orientation of the order parameter associated with the phase transition, can not be communicated between these regions and consequently will adopt different values. Examples are cosmic strings, magnetic monopoles, and domain walls. The defect density is thus given by the particle horizon in the early Universe. The defects are topologically stable, but time dependent motion leads to the emission of particles of mass comparable to the temperature at which the phase transition took place. The associated phase transition can also occur during reheating after inflation.

Alternatively, instead of being released from TDs, X particles may have been produced directly in the early Universe and, due to some unknown symmetries, have a very long lifetime comparable to the age of the Universe. In contrast to Weakly-Interacting Massive Particles (WIMPs) below a few hundred TeV which are the usual dark matter candidates motivated by, for example, supersymmetry and can be produced by thermal freeze out, such super-heavy X particles have to be produced non-thermally (see Ref. [84] for a review). In all these cases, such particles, also called “WIMPZILLAs”, would contribute to the dark matter and their decays could still contribute to UHECR fluxes today, with an anisotropy pattern that reflects the dark matter distribution in the halo of our Galaxy. However, these scenarios predict the absence of the GZK cutoff [85] and thus will be ruled out if the existence of the GZK cutoff is confirmed [8].

It is interesting to note that one of the prime motivations of the inflationary paradigm was to dilute excessive production of “dangerous relics” such as TDs and super-heavy stable particles. However, such objects can be produced right after inflation during reheating in cosmologically interesting abundances, and with a mass scale roughly given by the inflationary scale which in turn is fixed by the CMB anisotropies to  $\sim 10^{13}$  GeV [84]. The reader will realize that this mass scale is somewhat above the highest energies observed in CRs, which implies that the decay products of these primordial relics could well have something to do with UHECRs which therefore can probe such scenarios!

For dimensional reasons the spatially averaged X particle injection rate can only depend on the mass scale  $m_X$  and on cosmic time  $t$  in the combination

$$\dot{n}_X(t) = \kappa m_X^p t^{-4+p}, \quad (11)$$

where  $\kappa$  and  $p$  are dimensionless constants whose value depend on the specific top-down scenario [86]. For example, the case  $p = 1$  is representative of scenarios involving release of X particles from TDs, such as ordinary cosmic strings [87], monopoles connected by strings, so-called “necklaces” [88] and magnetic monopoles [89]. This can be easily seen as follows: The energy density  $\rho_s$  in a network of defects has to scale roughly as the critical density,  $\rho_s \propto \rho_{\text{crit}} \propto t^{-2}$ , where  $t$  is cosmic time, otherwise the defects would either start to over-close the Universe, or end up having a negligible contribution to the total energy density. In order to maintain this scaling, the defect network has to release energy with a rate given by  $\dot{\rho}_s = -a\rho_s/t \propto t^{-3}$ , where  $a = 1$  in the radiation dominated era, and  $a = 2/3$  during matter domination. If most of this energy goes into emission of X particles, then typically  $\kappa \sim \mathcal{O}(1)$ . In the numerical simulations presented below, it was assumed that the X particles are non-relativistic at decay.

The X particles could be gauge bosons, Higgs bosons, super-heavy fermions,

etc. depending on the specific GUT. They would have a mass  $m_X$  comparable to the symmetry breaking scale and would decay into leptons and/or quarks of roughly comparable energy. The quarks interact strongly and hadronize into nucleons ( $N$ s) and pions, the latter decaying in turn into  $\gamma$ -rays, electrons, and neutrinos. Given the  $X$  particle production rate,  $dn_X/dt$ , the effective injection spectrum of particle species  $a$  ( $a = \gamma, N, e^\pm, \nu$ ) via the hadronic channel can be written as  $(dn_X/dt)(2/m_X)(dN_a/dx)$ , where  $x \equiv 2E/m_X$ , and  $dN_a/dx$  is the relevant fragmentation function (FF).

The FFs are governed by quantum chromo dynamics (QCD). At energies reachable at accelerators the FFs have been measured in some detail. At the GUT scale energies relevant for top-down scenarios, however, extrapolations based on QCD have to be employed to obtain the FFs. In our calculations we adopt the Local Parton Hadron Duality (LPHD) approximation [90] according to which the total hadronic FF,  $dN_h/dx$ , is taken to be proportional to the spectrum of the partons (quarks/gluons) in the parton cascade (which is initiated by the quark through perturbative QCD processes) after evolving the parton cascade to a stage where the typical transverse momentum transfer in the QCD cascading processes has come down to  $\sim R^{-1} \sim$  few hundred MeV, where  $R$  is a typical hadron size. The parton spectrum is obtained from solutions of the standard QCD evolution equations in modified leading logarithmic approximation (MLLA) which provides good fits to accelerator data at LEP energies [90]. Within the LPHD hypothesis, the pions and nucleons after hadronization have essentially the same spectrum. The LPHD does not, however, fix the relative abundance of pions and nucleons after hadronization. Motivated by accelerator data, we assume the nucleon content  $f_N$  of the hadrons to be  $\simeq 10\%$ , and the rest pions distributed equally among the three charge states. Recent work on FFs goes beyond MLLA by solving the QCD evolution equations numerically and also includes the supersymmetric degrees of freedom at energies above the supersymmetry breaking scale [91]. The main difference in the results seems to be a nucleon-to-pion ratio that can be significantly higher at large  $x$  values for the extremely high energies of interest here [91]. However, the situation is not completely settled yet and the flux predictions are not very sensitive to such differences in the injection spectrum.

### 6.1 Predicted Fluxes

Fig. 7 shows results for the time averaged nucleon,  $\gamma$ -ray, and neutrino fluxes in a typical top-down scenario, along with constraints on diffuse  $\gamma$ -ray fluxes at GeV energies and neutrino flux sensitivities of future experiments. The spectrum was optimally normalized to allow for an explanation of the observed UHECR events, assuming their consistency with a nucleon or  $\gamma$ -ray

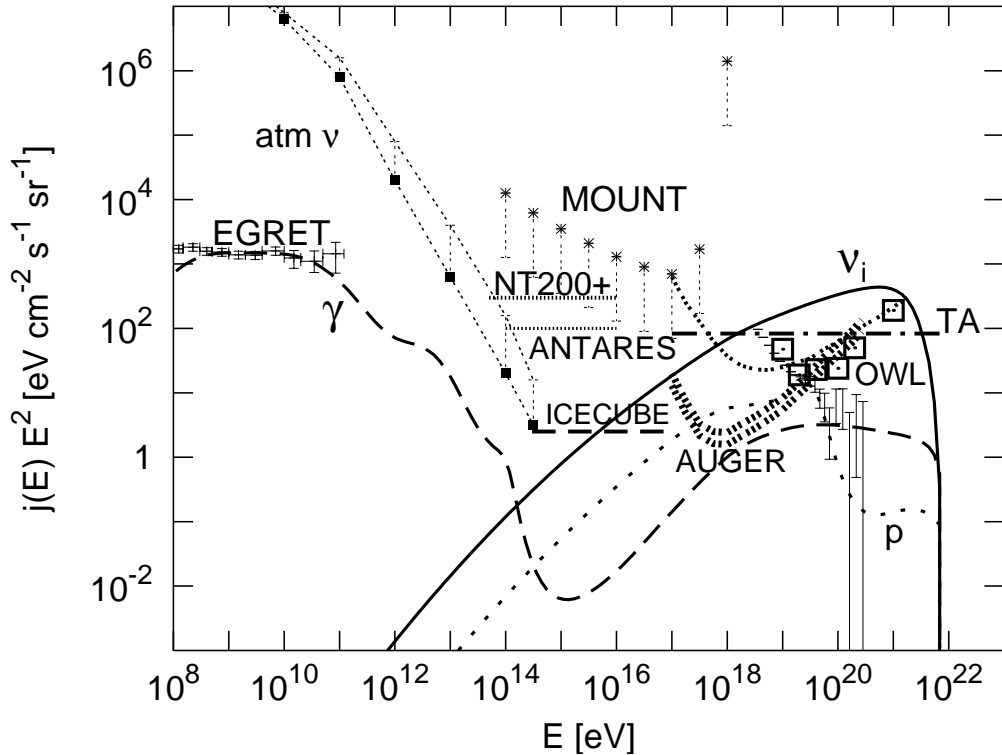


Fig. 7. [59] Predictions for the differential fluxes of  $\gamma$ -rays (dashed line), nucleons (dotted line), and neutrinos per flavor (solid line, assuming maximal mixing among all flavors) in a top-down model characterized by  $p = 1$ ,  $m_X = 2 \times 10^{14}$  GeV, and the decay mode  $X \rightarrow q + q$ , assuming the FF in MLLA without supersymmetry [90], with a fraction of 10% nucleons. The calculation used the code described in Ref. [28] and assumed the minimal URB version consistent with observations [36] and an EGMF of  $10^{-12}$  G. Measured CR, neutrino, and  $\gamma$ -ray data are as in Fig. 6 (however, only AGASA UHECR data are shown). Also shown are expected sensitivities of the currently being constructed Auger project to electron/muon and tau-neutrinos [92], and the planned projects telescope array (TA) [93], the fluorescence/Čerenkov detector MOUNT [94], and the space based OWL [95] (we take the latter as representative also for EUSO [96]), the water-based NT200+ [63], ANTARES [97], and the ice-based ICECUBE [98], as indicated.

primary. The flux below  $\lesssim 2 \times 10^{19}$  eV is presumably due to conventional acceleration in astrophysical sources and was not fit. The PP process on the CMB depletes the photon flux above 100 TeV, and the same process on the IR/O background causes depletion of the photon flux in the range 100 GeV–100 TeV, recycling the absorbed fluxes to energies below 100 GeV through EM cascading. The predicted background is *not* very sensitive to the specific IR/O background model, however [99]. The scenario in Fig. 7 obviously obeys all observational constraints within the normalization ambiguities. Note that the diffuse  $\gamma$ -ray background measured by EGRET [33] up to 10 GeV puts a strong constraint on these scenarios, especially if there is already a significant contribution to this background from conventional sources such as unresolved

$\gamma$ -ray blazars [100]. However, this constraint is much weaker for TDs or decaying long lived X particles with a non-uniform clustered density [101].

The energy loss and absorption lengths for UHE nucleons and photons are  $\lesssim 100$  Mpc. Thus, predicted UHE nucleon and photon fluxes are independent of cosmological evolution. The  $\gamma$ -ray flux below  $\simeq 10^{11}$  eV, however, scales as the total X particle energy release integrated over all redshifts and increases with decreasing  $p$  [102]. For  $m_X = 2 \times 10^{16}$  GeV, scenarios with  $p < 1$  are therefore ruled out, whereas models with a comovingly constant injection rate ( $p = 2$ ) are well within the limits.

It is clear from the above discussions that the predicted particle fluxes in the top-down scenarios are currently uncertain to a large extent due to particle physics uncertainties (e.g., mass and decay modes of the X particles, the quark FF, the nucleon fraction  $f_N$ , and so on) as well as astrophysical uncertainties (e.g., strengths of the radio and infrared backgrounds, extragalactic magnetic fields, etc.). More details on the dependence of the predicted UHE particle spectra and composition on these particle physics and astrophysical uncertainties are contained in Ref. [103].

We stress here that there are viable top-down scenarios which predict nucleon fluxes comparable to or even higher than the  $\gamma$ -ray flux at all energies, even though  $\gamma$ -rays dominate at injection. This occurs, e.g., in the case of high URB and/or for a strong EGMF, and a nucleon fraction of  $\simeq 10\%$ . Some of these top-down scenarios would therefore remain viable even if UHECR induced EAS should be proven inconsistent with photon primaries [104]). This is in contrast to scenarios with decaying massive dark matter in the Galactic halo which, due to the lack of interactions of injected particles, predict compositions directly given by the FFs, i.e. domination by  $\gamma$ -rays, and thus may be in conflict with observed compositions [104].

The normalization procedure to the UHECR flux described above imposes the constraint  $Q_{\text{UHECR}}^0 \lesssim 10^{-22}$  eV cm $^{-3}$  sec $^{-1}$  within a factor of a few [105,103,106] for the total energy release rate  $Q_0$  from TDs at the current epoch. In most top-down models, because of the unknown values of the parameters involved, it is currently not possible to calculate the exact value of  $Q_0$  from first principles, although it has been shown that the required values of  $Q_0$  (in order to explain the UHECR flux) mentioned above are quite possible for certain kinds of TDs. Some cosmic string simulations and the necklace scenario suggest that defects may lose most of their energy in the form of X particles and estimates of this rate have been given [107,88]. If that is the case, the constraint on  $Q_{\text{UHECR}}^0$  translates via Eq. (11) into a limit on the symmetry breaking scale  $\eta$  and hence on the mass  $m_X$  of the X particle:  $\eta \sim m_X \lesssim 10^{13}$  GeV [108]. Independently of whether or not this scenario explains UHECR, the EGRET measurement of the diffuse GeV  $\gamma$ -ray background leads to a similar bound,

$Q_{\text{EM}}^0 \lesssim 2.2 \times 10^{-23} h(3p - 1) \text{ eV cm}^{-3} \text{ sec}^{-1}$ , which leaves the bound on  $\eta$  and  $m_X$  practically unchanged. Furthermore, constraints from limits on CMB distortions and light element abundances from  $^4\text{He}$ -photo-disintegration are comparable to the bound from the directly observed diffuse GeV  $\gamma$ -rays [102]. That these crude normalizations lead to values of  $\eta$  in the right range suggests that defect models require less fine tuning than decay rates in scenarios of metastable massive dark matter. Furthermore, extragalactic top-down models would probably be less motivated, but not be ruled out automatically if the existence of the GZK cutoff is confirmed [8], in contrast to decaying massive dark matter scenarios.

As discussed above, in top-down scenarios most of the energy is released in the form of EM particles and neutrinos. If the X particles decay into a quark and a lepton, the quark hadronizes mostly into pions and the ratio of energy release into the neutrino versus EM channel is  $r \simeq 0.3$ . The energy fluence in neutrinos and  $\gamma$ -rays is thus comparable. However, whereas the photons are recycled down to the GeV range where their flux is constrained by the EGRET measurement, the neutrino flux is practically not changed during propagation and thus reflects the injection spectrum. Its predicted level is consistent with all existing upper limits (compare Fig. 7 with Fig. 6) but should be detectable by several experiments under construction or in the proposal stage (see Fig. 7). This would allow to directly see the quark fragmentation spectrum.

## 7 Experimental Projects and the Future

The field of ultra-high energy cosmic radiation is certainly experimentally driven. This is obvious from the lack of convergence of theoretical models caused by the sparseness of yet available data. To demonstrate the prospects for a considerable increase of data we therefore conclude with a short discussion of experimental projects.

An upscaled version of the old Fly's Eye experiment, the High Resolution Fly's Eye (HiRes) detector is looking for CRs in Utah, USA [8]. Taking into account a duty cycle of about 10% because a fluorescence detector requires clear, moonless nights, this instrument will collect events above  $10^{17}$  eV at a rate about 10 times larger than the old Fly's Eye, corresponding to a few events above  $10^{20}$  eV per year. The largest project presently under construction is the Pierre Auger Giant Array Observatory [21] planned for two sites, one in Mendoza, Argentina and another in Utah, USA for maximal sky coverage. Each site will have a  $\simeq 3000 \text{ km}^2$  ground array. The southern site will have about 1600 particle detectors (separated by 1.5 km each) overlooked by four fluorescence detectors. The ground arrays will have a duty cycle of nearly 100%, leading to detection rates about 30 times as large as for the AGASA

array, i.e. about 50 events per year above  $10^{20}$  eV. About 10% of the events will be detected simultaneously by the ground array and the fluorescence component and can be used for cross calibration and detailed EAS studies. The detection energy threshold will be around  $10^{18}$  eV. These instruments will also have considerable sensitivity to neutrinos above  $\sim 10^{19}$  eV, typically from the near-horizontal air-showers that are produced by them [92], as shown in Fig. 7. The old Fly's Eye experiment [65] and the AGASA experiment [64] have already established upper limits on neutrino fluxes based on the non-observation of horizontal air showers, see Fig. 6.

As Fig. 7 demonstrates for the top-down models, neutrino fluxes in the intermediate energy range from  $\simeq 10^{12}$  eV to  $\simeq 10^{15}$  eV can also be relevant for certain models including active galactic nuclei as CR sources. Traditionally, neutrinos in this range are detected via the EM showers or the Čerenkov light induced by the leptons produced by charged current reactions in ice or water. The largest operative experiment using ice is the Antarctic Muon And Neutrino Detector Array (AMANDA) [109] at the South pole which also has a next generation version named ICECUBE [98] which may reach up to  $\simeq 10^{18}$  eV. A water based version of this technique is operative in Lake Baikal [110] and another experiment for Astronomy with a Neutrino Telescope and Abyss environmental RESarch (ANTARES) is under construction in the Mediterranean [97].

In addition, there are plans to construct telescopes to detect fluorescence and Čerenkov light from near-horizontal showers produced in mountain targets by neutrinos in the intermediate window of energies between  $\sim 10^{15}$  eV and  $\sim 10^{19}$  eV [111,94]. The alternative of detecting neutrino and CR induced showers by triggering onto the radio pulses emitted by them is also investigated currently [112]. Two implementations of this technique, the Radio Ice Čerenkov Experiment (RICE), a small array of radio antennas in the South pole ice [66], and the Goldstone Lunar Ultra-high energy neutrino Experiment (GLUE), based on monitoring of the moon's rim with the NASA Goldstone radio telescope for radio pulses from neutrino-induced showers [67], have so far produced neutrino flux upper limits. It may be possible to use future large scale projects for radio telescopes such as the LOW Frequency ARray (LOFAR) for UHECR and neutrino studies of low energy and angular resolution but high statistics [113]. Acoustic detection of neutrino induced interactions is also being considered [114].

There are also plans to detect EAS in the Earth's atmosphere from space. This would provide an increase by another factor  $\sim 50$  in collecting power compared to the Pierre Auger Project, i.e. an event rate above  $10^{20}$  eV of up to a few thousand per year. Two concepts are currently being studied, the Orbiting Wide-angle Light-collector (OWL) [95] in the USA and the Extreme Universe Space Observatory (EUSO) [96] in Europe of which a prototype may



fly on the International Space Station.

Space-based detectors would be especially suitable for detection of very small event rates such as those caused by neutrino primaries which rarely interact in the atmosphere due to their small interaction cross sections. This disadvantage for the detection process is at the same time a blessing because it makes these elusive particles reach us unattenuated over cosmological distances and from very dense environments where all other particles (except gravitational waves) would be absorbed. Giving rise to showers typically starting deep within the atmosphere, they can also be distinguished from other primaries.

We believe that these experimental developments will allow to test, constrain, or rule out many of the theoretical scenarios and speculations discussed here. This will begin already within the next few years.

## Acknowledgments

I would like to thank all my collaborators without whose contributions and help this review would have been impossible.

## References

- [1] V. F. Hess, *Phys. Z.* 13 (1912) 1084.
- [2] P. Auger, R. Maze, T. Grivet-Meyer, *Académie des Sciences* 206 (1938) 1721; P. Auger, R. Maze, *ibid.* 207 (1938) 228.
- [3] for a general introduction on cosmic rays see, e.g., V. S. Berezinsky, S. V. Bulanov, V. A. Dogiel, V. L. Ginzburg, V. S. Ptuskin, *Astrophysics of Cosmic Rays* (North-Holland, Amsterdam, 1990); T. K. Gaisser, *Cosmic Rays and Particle Physics*, Cambridge University Press (Cambridge, 1998).
- [4] for a recent overview see, e.g., R. Battiston, e-print astro-ph/0208108.
- [5] See, e.g., M. A. Lawrence, R. J. O. Reid, and A. A. Watson, *J. Phys. G Nucl. Part. Phys.* 17 (1991) 733, and references therein; see also <http://ast.leeds.ac.uk/haverah/hav-home.html>.
- [6] M. Takeda et al., *Phys. Rev. Lett.* 81 (1998) 1163; *Astrophys. J.* 522 (1999) 225; Hayashida et al., e-print astro-ph/0008102; see also <http://www-akeno.icrr.u-tokyo.ac.jp/AGASA/>.
- [7] D. J. Bird et al., *Phys. Rev. Lett.* 71 (1993) 3401; *Astrophys. J.* 424 (1994) 491; *ibid.* 441 (1995) 144.

- [8] T. Abu-Zayyad et al. (HiRes collaboration), e-print astro-ph/0208243; e-print astro-ph/0208301.
- [9] for recent reviews see J. W. Cronin, Rev. Mod. Phys. 71 (1999) S165; M. Nagano, A. A. Watson, Rev. Mod. Phys. 72 (2000) 689; A. V. Olinto, Phys. Rept. 333-334 (2000) 329; X. Bertou, M. Boratav, and A. Letessier-Selvon, Int. J. Mod. Phys. A15 (2000) 2181; G. Sigl, Science 291 (2001) 73.
- [10] P. Bhattacharjee and G. Sigl, Phys. Rept. 327 (2000) 109; L. Anchordoqui, T. Paul, S. Reucroft, and J. Swain, e-print hep-ph/0206072.
- [11] “Physics and Astrophysics of Ultra High Energy Cosmic Rays”, Lecture Notes in Physics, vol. 576 (Springer Verlag, 2001), eds. M. Lemoine, G. Sigl.
- [12] A. M. Hillas, Ann. Rev. Astron. Astrophys. 22 (1984) 425.
- [13] G. Sigl, D. N. Schramm, and P. Bhattacharjee, Astropart. Phys. 2 (1994) 401.
- [14] C. A. Norman, D. B. Melrose, and A. Achterberg, Astrophys. J. 454 (1995) 60.
- [15] K. Greisen, Phys. Rev. Lett. 16 (1966) 748; G. T. Zatsepin and V. A. Kuzmin, Pis'ma Zh. Eksp. Teor. Fiz. 4 (1966) 114 [JETP. Lett. 4 (1966) 78].
- [16] see, e.g., M. Blanton, P. Blasi, and A. V. Olinto, Astropart. Phys. 15 (2001) 275.
- [17] J. L. Puget, F. W. Stecker, and J. H. Bredekamp, Astrophys. J. 205 (1976) 638; L. N. Epele and E. Roulet, Phys. Rev. Lett. 81 (1998) 3295; J. High Energy Phys. 9810 (1998) 009; F. W. Stecker, Phys. Rev. Lett. 81 (1998) 3296; F. W. Stecker and M. H. Salamon, Astrophys. J. 512 (1999) 521.
- [18] J. W. Elbert, and P. Sommers, Astrophys. J. 441 (1995) 151.
- [19] P. G. Tinyakov and I. I. Tkachev, Pisma Zh. Eksp. Teor. Fiz. 74 (2001) 3 [JETP Lett. 74 (2001) 1].
- [20] for a discussion see, e.g., J. N. Bahcall and E. Waxman, e-print hep-ph/0206217.
- [21] J. W. Cronin, Nucl. Phys. B (Proc. Suppl.) 28B (1992) 213; The Pierre Auger Observatory Design Report (ed. 2), March 1997; see also <http://www.auger.org>.
- [22] for a recent review, see F. Halzen and D. Hooper, Rept. Prog. Phys. 65 (2002) 1025.
- [23] R. A. Ong, Phys. Rept. 305 (1998) 95; M. Catanese and T. C. Weekes, e-print astro-ph/9906501, invited review, Publ. Astron. Soc. of the Pacific, Vol. 111, issue 764 (1999) 1193.
- [24] E. Waxman and J. Bahcall, Phys. Rev. D. 59 (1999) 023002; J. Bahcall and E. Waxman, Phys. Rev. D 64 (2001) 023002.
- [25] Proc. 19<sup>th</sup> Texas Symposium on Relativistic Astrophysics, Paris (France), eds. E. Aubourg, et al., Nuc. Phys. B (Proc. Suppl.) 80B (2000).

- [26] K. Mannheim, R. J. Protheroe, J. P. Rachen, Phys. Rev. D 63 (2001) 023003; J. P. Rachen, R. J. Protheroe, K. Mannheim, astro-ph/9908031, in Ref. [25].
- [27] for more details see, e.g., G. Sigl, in Ref. [11], pp. 196-254.
- [28] S. Lee, Phys. Rev. D 58 (1998) 043004; O. E. Kalashev, V. A. Kuzmin, and D. V. Semikoz, e-print astro-ph/9911035; Mod. Phys. Lett A16 (2001) 2505.
- [29] O. E. Kalashev, V. A. Kuzmin, D. V. Semikoz, and G. Sigl, Phys. Rev. D 65 (2002) 103003.
- [30] O. E. Kalashev, V. A. Kuzmin, D. V. Semikoz, and G. Sigl, Phys. Rev. D 66 (2002) 063004.
- [31] T. J. Weiler, Phys. Rev. Lett. 49 (1982) 234; Astrophys. J. 285 (1984) 495; E. Roulet, Phys. Rev. D 47 (1993) 5247; S. Yoshida, Astropart. Phys. 2 (1994) 187.
- [32] T. J. Weiler, Astropart. Phys. 11 (1999) 317; D. Fargion, B. Mele, and A. Salis, Astrophys. J. 517 (1999) 725; S. Yoshida, G. Sigl, and S. Lee, Phys. Rev. Lett. 81 (1998) 5505; Z. Fodor, S. D. Katz, and A. Ringwald, Phys. Rev. Lett. 88 (2002) 171101.
- [33] P. Sreekumar et al., Astrophys. J. 494 (1998) 523.
- [34] V. Berezhinsky, M. Kachelrieß, and S. Ostapchenko, e-print hep-ph/0205218.
- [35] T. A. Clark, L. W. Brown, and J. K. Alexander, Nature 228 (1970) 847.
- [36] R. J. Protheroe and P. L. Biermann, Astropart. Phys. 6 (1996) 45.
- [37] J. R. Primack, R. S. Somerville, J. S. Bullock, and J. E. Devriendt, e-print astro-ph/0011475, AIP Conf. Proc. 558 (2001) 463.
- [38] for a review see, e.g., D. Grasso and H. Rubinstein, Phys. Rept. 348 (2001) 163.
- [39] J. P. Vallée, Fundamentals of Cosmic Physics, Vol. 19 (1997) 1; J.-L. Han and R. Wielebinski, e-print astro-ph/0209090.
- [40] D. Ryu, H. Kang, and P. L. Biermann, Astron. Astrophys. 335 (1998) 19.
- [41] P. Blasi, S. Burles, and A. V. Olinto, Astrophys. J. 514 (1999) L79.
- [42] G. Medina-Tanco and T. Enßlin, Astropart. Phys. 16 (2001) 47.
- [43] E. Waxman and J. Miralda-Escudé: Astrophys. J. 472 (1996) L89.
- [44] C. Isola and G. Sigl, e-print astro-ph/0203273.
- [45] F. Miniati, e-print astro-ph/0203014.
- [46] T. Enßlin, F. Miniati, and G. Sigl, in preparation.
- [47] J. Alvarez-Muñiz, R. Engel, and T. Stanev, Astrophys. J. 572 (2001) 185.
- [48] G. Bertone, C. Isola, M. Lemoine, and G. Sigl, e-print astro-ph/0209192.

- [49] D. S. Gorbunov, G. G. Raffelt, and D. V. Semikoz, *Phys. Rev. D* 64 (2001) 096005.
- [50] G. R. Farrar, *Phys. Rev. Lett.* 76 (1996) 4111; D. J. H. Chung, G. R. Farrar, and E. W. Kolb, *Phys. Rev. D* 57 (1998) 4696.
- [51] I. F. Albuquerque et al. (E761 collaboration), *Phys. Rev. Lett.* 78 (1997) 3252; A. Alavi-Harati et al. (KTeV collaboration), *Phys. Rev. Lett.* 83 (1999) 2128.
- [52] P. G. Tinyakov and I. I. Tkachev, *JETP Lett.* 74 (2001) 445; D. S. Gorbunov, P. G. Tinyakov, I. I. Tkachev, and S. V. Troitsky, e-print astro-ph/0204360.
- [53] R. Gandhi, C. Quigg, M. H. Reno, and I. Sarcevic, *Astropart. Phys.* 5 (1996) 81; *Phys. Rev. D* 58 (1998) 093009.
- [54] G. Domokos and S. Kovesi-Domokos, *Phys. Rev. Lett.* 82 (1999) 1366.
- [55] N. Arkani-Hamed, S. Dimopoulos, and G. Dvali, *Phys. Lett. B* 429 (1998) 263; I. Antoniadis, N. Arkani-Hamed, S. Dimopoulos, and G. Dvali, *Phys. Lett. B* 436 (1998) 257; N. Arkani-Hamed, S. Dimopoulos, and G. Dvali, *Phys. Rev. D* 59 (1999) 086004.
- [56] E.-J. Ahn, M. Cavaglia, and A. V. Olinto, e-print hep-th/0201042.
- [57] J. L. Feng and A. D. Shapere, *Phys. Rev. Lett.* 88 (2002) 021303.
- [58] M. Kachelrieß and M. Plümacher, *Phys. Rev. D* 62 (2000) 103006.
- [59] I acknowledge Dmitry Semikoz for helping me with these figures which are based on work in Ref. [30].
- [60] see, e.g., P. Lipari, *Astropart. Phys.* 1, 195 (1993).
- [61] For general information see <http://wsgs02.lngs.infn.it:8000/macro/>; see also M. Ambrosio *et al.* [MACRO Collaboration], astro-ph/0203181.
- [62] J. Ahrens et al., AMANDA collaboration, e-print hep-ph/0112083, Proceedings of the EPS International Conference on High Energy Physics, Budapest, 2001 (D. Horvath, P. Levai, A. Patkos, eds.), JHEP Proceedings Section, PrHEP-hep2001/207.
- [63] V. Balkanov *et al.* [BAIKAL Collaboration], astro-ph/0112446.
- [64] S. Yoshida for the AGASA Collaboration, *Proc. of 27th ICRC (Hamburg)* 3 (2001) 1142.
- [65] R. M. Baltrusaitis et al., *Astrophys. J.* 281 (1984) L9; *Phys. Rev. D* 31 (1985) 2192.
- [66] I. Kravchenko et al. (RICE collaboration), e-print astro-ph/0206371; for general information on RICE see <http://kuhep4.phsx.ukans.edu/iceman/index.html>.
- [67] P. W. Gorham, K. M. Liewer, C. J. Naudet, e-print astro-ph/9906504, *Proc. of the 26th International Cosmic Ray Conference (ICRC 99), Salt Lake City, Utah*, Vol. 2, p. 479; P. W. Gorham et al., e-print astro-ph/0102435.

- [68] D. A. Morris and A. Ringwald, *Astropart. Phys.* 2 (1994) 43.
- [69] C. Tyler, A. Olinto, and G. Sigl, *Phys. Rev. D* 63 (2001) 055001.
- [70] see, e.g., L. A. Anchordoqui, J. L. Feng, H. Goldberg, and A. D. Shapere, *Phys. Rev. D* 65 (2002) 124027; e-print hep-ph/0207139.
- [71] A. Kusenko and T. Weiler, *Phys. Rev. Lett.* 88 (2002) 161101.
- [72] G. Dvali, G. Gabadadze, M. Kolanović, and F. Nitti, *Phys. Rev. D* 65 (2001) 024031.
- [73] G. Dvali, G. Gabadadze, and M. Shifman, e-print hep-th/0202174.
- [74] G. Sigl, e-print hep-ph/0207254.
- [75] H. Sato and T. Tati, *Prog. Theor. Phys.* 47 (1972) 1788; D. A. Kirzhnits and V. A. Chechin, *Sov. J. Nucl. Phys.* 15 (1972) 585; L. Gonzalez-Mestres, e-print hep-th/0208064.
- [76] S. Coleman and S. L. Glashow, *Phys. Lett.* B405 (1997) 249; *Phys. Rev. D* 59 (1999) 116008.
- [77] G. Amelino-Camelia and T. Piran:, *Phys. Lett.* B497 (2001) 265.
- [78] J. Magueijo and L. Smolin, e-print gr-qc/0207085.
- [79] D. Colladay and V. Kostelecky, *Phys. Rev. D* 59 (1999) 116002.
- [80] see, e.g., J. Ellis, N. E. Mavromatos, and D. V. Nanopoulos, *Phys. Rev. D* 62 (2000) 084019.
- [81] R. Aloisio, P. Blasi, P. Ghia, and A. Grillo, *Phys. Rev. D* 62 (2000) 053010.
- [82] see, e.g., R. Protheroe and H. Meyer, *Phys. Lett.* B493 (1996) 1; S. Liberati, T. Jacobson, and D. Mattingly, e-print hep-ph/0112207.
- [83] T. Jacobson, S. Liberati, and D. Mattingly, e-print hep-ph/0209264.
- [84] for a brief review see V. Kuzmin and I. Tkachev, *Phys. Rept.* 320 (1999) 199
- [85] V. Berezhinsky, M. Kachelrieß , and A. Vilenkin, *Phys. Rev. Lett.* 79 (1997) 4302.
- [86] P. Bhattacharjee, C. T. Hill, and D. N. Schramm, *Phys. Rev. Lett.* 69 (1992) 567.
- [87] see, e.g., P. Bhattacharjee and N. C. Rana, *Phys. Lett.* B 246 (1990) 365.
- [88] V. Berezhinsky and A. Vilenkin, *Phys. Rev. Lett.* 79 (1997) 5202.
- [89] P. Bhattacharjee and G. Sigl, *Phys. Rev. D* 51 (1995) 4079 .
- [90] Yu. L. Dokshitzer, V. A. Khoze, A. H. Müller, and S. I. Troyan, *Basics of Perturbative QCD* (Editions Frontieres, Singapore, 1991).

- [91] see, e. g., S. Sarkar and R. Toldrà, Nucl. Phys. B 621 (2002) 495; C. Barbot and M. Drees, Phys. Lett. B 533 (2002) 107.
- [92] J. J. Blanco-Pillado, R. A. Vázquez, and E. Zas, Phys. Rev. Lett. 78 (1997) 3614; K. S. Capelle, J. W. Cronin, G. Parente, and E. Zas, Astropart. Phys. 8 (1998) 321; A. Letessier-Selvon, e-print astro-ph/0009444, AIP Conf. Proc 566 (2000) 157; X. Bertou et al., Astropart. Phys. 17 (2002) 183.
- [93] M. Sasaki and M. Jobashi, e-print astro-ph/0204167.
- [94] G. W. S. Hou and M. A. Huang, astro-ph/0204145.
- [95] D. B. Cline and F. W. Stecker, OWL/AirWatch science white paper, e-print astro-ph/0003459.
- [96] See <http://www.ifcai.pa.cnr.it/lfcai/euso.html>.
- [97] For general information see <http://antares.in2p3.fr>; see also S. Basa, (e-print astro-ph/9904213, in [25]; ANTARES Collaboration, e-print astro-ph/9907432.
- [98] For general information see <http://www.ps.uci.edu/~icecube/workshop.html>; see also F. Halzen: Am. Astron. Soc. Meeting 192, # 62 28 (1998); AMANDA collaboration: astro-ph/9906205, Proc. 8<sup>th</sup> International Workshop on Neutrino Telescopes, Venice, Feb. 1999.
- [99] P. S. Coppi and F. A. Aharonian, Astrophys. J. 487 (1997) L9.
- [100] R. Mukherjee and J. Chiang, Astropart. Phys. 11 (1999) 213.
- [101] V. Berezhinsky, M. Kachelrieß, and A. Vilenkin, Phys. Rev. Lett. 79 (1997) 4302.
- [102] G. Sigl, K. Jedamzik, D. N. Schramm, and V. Berezhinsky, Phys. Rev. D 52 (1995) 6682.
- [103] G. Sigl, S. Lee, P. Bhattacharjee, and S. Yoshida, Phys. Rev. D 59 (1999) 043504.
- [104] M. Ave et al., Phys. Rev. D 65 (2002) 063007; K. Shinozaki et al. (AGASA collaboration), Astrophys. J. 571 (2002) L117.
- [105] R. J. Protheroe and T. Stanev, Phys. Rev. Lett. 77 (1996) 3708; erratum, ibid. 78 (1997) 3420.
- [106] G. Sigl, S. Lee, D. N. Schramm, and P. S. Coppi, Phys. Lett. B 392 (1997) 129.
- [107] G. R. Vincent, N. D. Antunes, and M. Hindmarsh, Phys. Rev. Lett. 80 (1998) 2277; G. R. Vincent, M. Hindmarsh, and M. Sakellariadou, Phys. Rev. D 56 (1997) 637.
- [108] U. F. Wichoski, J. H. MacGibbon, and R. H. Brandenberger, Phys. Rev. D 65 (2002) 063005.

- [109] For general information see <http://amanda.berkeley.edu/>; see also F. Halzen: *New Astron. Rev* 42 (1999) 289; for recent physics results see, e.g., J. Ahrens et al. (AMANDA Collaboration), e-print astro-ph/0206487; e-print astro-ph/0208006.
- [110] For general information see <http://www-zeuthen.desy.de/baikal/baikalhome.html>; see also V. Balkanov et al (Baikal Collaboration), Proceedings of the IX International Workshop on Neutrino Telescopes, Venezia, March 6-9, 2001, Vol.II, p.591 (Ed. M.Balda-Ceolin).
- [111] see, e.g., D. Fargion, e-print hep-ph/0111289.
- [112] Proceedings of *First International Workshop on Radio Detection of High-Energy Particles*, Amer. Inst. of Phys., vol. 579 (2001), and at <http://www.physics.ucla.edu/moonemp/radhep/workshop.html>; see also K. Green, J. L. Rosner, D. A. Suprun, and J. F. Wilkerson, e-print astro-ph/0205046.
- [113] H. Falcke and P. Gorham, e-print astro-ph/0207226.
- [114] see, e.g., L. G. Dedenko, I. M. Zheleznykh, S. K. Karaevsky, A. A. Mironovich, V. D. Svet and A. V. Furduev, *Bull. Russ. Acad. Sci. Phys.* 61 (1997) 469 [*Izv. Ross. Akad. Nauk.* 61 (1997) 593].